MethodsX 9 (2022) 101771

Contents lists available at ScienceDirect

MethodsX

journal homepage: www.elsevier.com/locate/mex

Method Article

The role of eugenol and ferulic acid as the competitive inhibitors of transcriptional regulator RhlR in *P. aeruginosa*

Esmeralda Escobar-Muciño

Postgrado en ciencias ambientales, Instituto Potosino de Investigación Científica y Tecnológica A.C (IPICYT). Camino a la Presa San José No. 2055. Col. Lomas 4ª. Sección, San Luis Potosí C.P. 78216, México

A B S T R A C T

Search inhibitors of Quorum Sensing (QS) in *Pseudomonas aeruginosa* are challenging to find therapies due to the broad antibiotic resistance. Therefore, this study aimed to probe ten aromatic compounds as inhibitors of three transcriptional regulators of QS in *P. aeruginosa*. The methodology consisted in determining the Binding Gibbs Energy (BGE) with software Chimera (tool vina) and Mcule, comparing the averages by the Tukey method ($p \leq 0.05$) to find inhibitors of QS. Subsequently, the LD_{50} in the mice model was evaluated by three QSAR models, and the *in silico* pharmacokinetic values were obtained from the ADME (the absorption distribution metabolism excretion) and PubChem databases. Found three potential inhibitors of RhlR with the lower BGE values in the range -6.70±0.21 to -7.43±0.35 kcal/mol. On the other side, all compounds were acceptable for Lipinski's rule of fives and the *in silico* oral mice LD_{50} and ADME values. Concluding, the ferulic acid and eugenol showed the best total BGE values (-75.07±0.892 and -70.36±1.022 kcal/mol), proposing them as a new therapy against the virulence of *P. aeruginosa*. Finally, the *in silico* studies have demonstrated are reproducible and valuable for putative QS inhibitors predicting and obtaining new studies derivatives from the results obtained in the present study.

- The key benefits of this methodology are:

Use free, licensed, flexible, and efficient software for *in silico* molecular docking.

- Validation and comparison of BGE employing two molecular docking software in three different proteins.
- Use classical molecular dynamics to define the stability and the total BGE of interaction protein-ligand and find the best inhibitor of a protein for proposing them as a possible therapy against the virulence of specific pathogens.

E-mail address: esmeralda.escobar@ipicyt.edu.mx

https://doi.org/10.1016/j.mex.2022.101771

ARTICLE INFO
Method name: Identification of potential quorum sensing protein regulator inhibitors by molecular docking screening and classic molecular dynamic
Keywords: Molecular docking, Quorum sensing inhibitors, validation Validation of software, Molecular dynamic, therapy, virulence, and Gram-negative bacteria
Article history: Available online 23 June 2022

Specifications table

Subject Area;	Bioinformatics
More specific subject area;	Biomolecular simulations, structural bioinformatics, systems biology, and inhibition mechanism for disease-causing microorganisms
Method name;	Identification of potential quorum sensing protein regulator inhibitors by molecular docking screening and classic molecular dynamic
Name and reference of the original method;	N.A.
Resource availability;	N.A.

Method details

Background

Gram-negative bacteria use Quorum Sensing (QS) systems to monitor their local environment and population density by producing, secreting, and detecting small diffusible signals called autoinducers, resulting in synchronous regulation of gene expression of the entire population [1].

Autoinducer molecules play crucial roles in signal transduction. When an autoinducer molecule reaches a certain concentration threshold, it can coordinate the expression of multiple genes, leading to changes in the behavior of the bacterial population by activating regulatory proteins in response to this signal. Gram-negative bacteria produce a wide range of signal molecules that have been identified and characterized [2,3]. The acyl-homoserine lactone (AHL_S) has an acyl side-chain that varies from C_4 to C_{18}; they are usually straight and, in some cases, may have a branched configuration [3].

On the other hand, the bacterial pathogen *P. aeruginosa* activates the expression of many virulence genes in a cell density-dependent manner by using an intricate QS network. *P. aeruginosa* has two acyl-homoserine-lactone canonical QS systems (LasI/LasR and RhlI-RhlR) and a non-canonical system known as LuxR-solo (QscR). In the case of LasI/LasR, this QS activates many genes, including those involved in the production of the molecule N-3-oxo-dodecanoyl-L-homoserine lactone (3-oxo-C_{12}-AHL), as well as those participating in the regulation of various virulence factors such as *lasA* (staphylidosin), *lasB* (elastase), *aprA* (alkaline protease), *toxA* (exotoxin A), and *hcnABC* (hydrogen cyanide synthase) [4–6]. By contrast, the second canonical QS system RhlI/RhlR participates in the synthesis of n-butyryl-l-homoserine lactone (C_4-AHL), in the regulation of receptor transcription RhlR and other genes, such as *lasB* (elastase B), *rhlAB* (rhamnolipid synthesis genes), *rhlI* (autoinducer synthase), *rpoS* (the stationary phase sigma factor), *lecA* (type 1 lectin), *lecB* (type II lectin) and *hcnABC.* The QS system RhlI/RhlR also modulates genes involved in pyocyanin production [4–6].

The aromatic compounds proposed for the present study are primarily microbial bioconversion products (catechol and protocatechuate) and subproducts obtained from bacterial bioconversion. In the specific case of the transformation of ferulic acid to obtain three principal bioproducts (vanillic acid, vanillin, and vanillic alcohol), and for other instances, the use of essential oils, such as eugenol and isoeugenol, has been suggested [7–10]. In addition, some aromatic compounds that participate in the β-ketoadipate pathway, such as hydroxybenzaldehyde and p-hydroxybenzoic acid, are safe for human consumption by the Food Drugs and Administration (FDA) [7–11]. These compounds have protective effects, bioactive, anticancer, antioxidant, anti-inflammatory properties, antiviral and antibacterial activities. In addition, QS inhibitory properties have been reported in some Gram-negative microorganisms, such as *P. aeruginosa* [12–16].

Furthermore, the publication of new three-dimensional structural proteins and the development of tools for obtaining 3D protein models by modeling homology have allowed validation of the tridimensional structures of many proteins. These results have been achieved by getting the sequence of amino acids from the NCBI databases in FASTA format. Therefore, the *in silico* methods have made it possible to discover, in various microorganisms, an endless number of QS inhibitory molecules, such as different aromatic compounds, for instance, tyrosol halogenated furanone, coumarins, flavones, and their derivatives [17–23]. Molecular docking software is currently used for validation by docking and re-docking protocols, either as licensed or free software (e.g., Autodock vina, Autodock4, LeDock, GOLD, Chimera, Mcule, and PyRx) [21,24,25].

With the resulting information, key player amino acids have been identified, involved in the binding of inhibitory molecules with the autoinducer-1 binding domain, which allows the binding of various transcriptional regulators in pathogenic bacteria. This information serves to create point mutations in the QS transcriptional regulators to understand the biological role of amino acids in the protein-ligand binding. Likewise, gene cloning is related to the synthesis of new molecules and increases the affinity to the autoinducer-1 binding domain in the transcriptional regulator of QS obtained, thus attenuating bacterial virulence regulated by QS [19].

Nowadays, researchers have turned their attention to obtaining the pharmacokinetic properties of thousands of compounds to characterize them based on platforms such as Swiss-ADME (http://www.swissadme.ch/) [26]. In addition, Lipinski's Rule of Five has been used for early research on drug discovery. This rule correlates physicochemical properties, such as aqueous solubility, permeability, and oral bioavailability of many molecules. Subsequently, the FDA must approve a candidate molecule by evaluating the results obtained from *in vitro* and *in vivo* experiments, the subsequent clinical protocols, and the use of good manufacturing practices for drugs (GMP) [27]. In addition, GROMACS and NAMD software help perform complementary molecular dynamics validation assays. Classical molecular dynamics consists of several steps: (i) producing protein topologies, (ii) defining the shape of the box to solvate a protein, (iii) adding ions to neutralize charges, thus minimizing the energy of the system under certain study conditions, and (iv) balancing the system based on the physicochemical properties (such as temperature, volume, density, and pressure) when the protein interacts with its ligands [28,29]. This software helps to obtain the molecular dynamics of a protein and observe its stability (without interacting with its ligand) and the interactions with ligands evaluated during a 50-100 ns. Also, GROMACS and NAMD find stable interactions over the monitored time by calculating and analyzing variables such as the Root Mean Square Deviation (RMSD) and Root-Mean-Square Fluctuation (RMSF). Other necessary calculations in molecular dynamics experiments are: (i) solvent accessible surface area (SASA), (ii) percentage of amino acid residues involved in protein binding, and (iii) radius of gyration stability. All these parameters help to compare protein-ligand interactions from a molecular docking screening showing the ligands that may or may not favor the activity of a protein [28]. Finally, the free energy of binding of a protein-ligand system can be known by estimating the average molecular by, "Molecular Mechanics/Generalized Born Surface Area (MM/GBSA)" method [30].

Therefore, this work aimed to search for QS inhibitors employing a molecular docking study of ten aromatic compounds by describing how to inhibit the three main transcriptional regulators of QS (LasR, RhlR, and QscR) in *P. aeruginosa.* Comparing the binding energy of two inhibitors of QS (furanone C30 and vanillin) reported by other authors. Also, were described the key player amino acids from the transcriptional regulator of QS when they bind to functional groups from a specific inhibitor to compare with the key player amino acids of each transcriptional regulator when they bind to their natural ligands (C_{12}-AHL, C_4-AHL, and C_{10}-AHL). Finally, a classical molecular dynamics study was proposed for validating the results of molecular docking of transcriptional regulators with each inhibitor, which helped suggest a therapy against virulent *P. aeruginosa* regulated by the QS mechanism.

Methodology

Inhibitors and regulator transcriptional proteins

SMILE codes and files with the SDF extension of all aromatic compounds were manually obtained from the PubChem database. Subsequently, the three-dimensional structures of LasR (PDB ID 3IX3) and QscR (PDB ID 6CBQ) were obtained from the PDB platform. These PDB files were used as a template for the molecular docking test, getting the Binding Gibbs Energy (BGE) or ΔG expressed in -kcal/mol for each protein-ligand interaction of the transcriptional regulator LasR with the ten aromatic compounds. For the above, two molecular docking software was employed, Mcule and UCSF Chimera, as explained in the corresponding section [24,25]. Finally, PyMol (version 4.60) and Discovery Studio (version 2020) were used to know the coordinates of the binding domain of each transcriptional regulator [31,32].

The homology modeling of the RhlR protein

Because the three-dimensional structure of transcriptional regulator RhlR was not in the Protein Data Bank (PDB), the RhlR protein sequence was obtained from NCBI in FASTA format (ID: WP_003119559.1). The homology method modeled these 241 amino acids sequence in SWISS-MODEL to find a protein homologous to RhlR, whose function was related to the QS in bacteria. Moreover, the scoring function was used from the SWISS-MODEL platform to estimate the overall quality of the RhlR three-dimensional model [23]. Subsequently, all the water molecules and heteroatoms were removed, and the RhlR model validation analysis was completed in the RAMPAGE Ramachandran plot analysis server (https://zlab.umassmed.edu/bu/rama) [33]. The SdiA three-dimensional structure from *E. coli* (PDB: 4y15.2.A) was the reference structure used to obtain the model for the RhlR protein. Also, PDB formats for SdiA and RhlR regulators were uploaded to the ProSA server. Then, each protein's A chain was analyzed, and Z score values for both proteins were obtained (https://prosa.services.came.sbg.ac.at/prosa.php) [34]. The quality of the three-dimensional structure of RhlR was compared with the three-dimensional structure of the transcriptional regulator SdiA published in PDB. Finally, the regulatory proteins were loaded into the Chimera software to match both crystals employing the "Matchmaker" tool, and the transcriptional regulators were very similar in structure and folding.

Three RhlR models were generated by MODELLER software, and the best structure was chosen based on the MODELLER DOPE score (-27092.129) in comparison with the SdiA protein DOPE score (-29141.43) [35]. Finally, the best protein model was tested in the PROCHECK server and was found acceptable results for all characteristics measured and validation of protein-structure coordinates (https://saves.mbi.ucla.edu/) [36].

Molecular docking and molecular dynamics

The three-dimensional structures of the transcriptional regulators (LasR and QscR) were obtained from the Protein Data Bank (PDB) database with a PDB code for 3IX3 and 6CBQ for the QscR transcriptional regulator. Subsequently, the natural ligands of LasR and QscR, C_{12}-AHL, and C_{10}-AHL were removed from the protein regulators of QS using the Pymol program [31]. Afterward, the three regulator proteins were prepared and saved in PDB format for the molecular docking test, employing different software to predict the BGE of each protein, using the ten aromatic compounds proposed as ligands. The ligand-binding domain selection box (grid-box) was generated by locating the residues of the AHL binding domain. For each transcriptional regulator was obtained different coordinates: LasR (X: 40.491, Y: 9.8455, and Z: 7.345 Å), QscR (X: -77.418, Y: -4.841 and Z: 9.181 Å) and RhlR (X: 4.83, Y: 64.94, and Z: 40.89 Å) [37]. The interaction of each transcriptional regulator with the corresponding functional groups from the aromatic compounds was described for the bonds formed between the ligand and each regulatory protein. Also, molecular docking was performed to simulate biological conditions in the presence of neutralizing molecules [24]. BGE values were obtained from

three runs in each software and plotted in Excel, and all data were categorized based on ten aromatic compound results.

Moreover, the comparison of results was carried on with the average BGE values obtained for LasR (ΔG =-7.86±0.19 kcal/mol), QscR (ΔG=-7.53±0.07 kcal/mol), and RhlR (ΔG=-5.51±0.02 kcal/mol). On the other hand, the results from aromatic compounds were compared according to the binding energy obtained from each interaction. Furthermore, the results obtained from molecular docking of the three transcriptional regulators of *P. aeruginosa* with two inhibitors of QS were for furanone: -4.2 to -4.9 kcal/mol and for vanillin: -6.2 to -6.77 kcal/mol. These analyses contribute to finding the ligand that acts as the best inhibitor by selecting the molecule with the lowest binding energy [14,38,39].

Molecular dynamics analysis was conducted to validate the optimal molecular dockings based on the best results. The RMSD, RMSF, and SASA graphs for 50 ns were obtained to determine the protein and ligand stability. The percentages of amino acids most frequently present in the best-performing interactions were also determined [28,29]. Finally, the total binding energy was obtained by NAMD software through the method called "Generalized Born Surface Area of average Molecular Mechanics (MM/GBSA)" [30].

Ligand preparation

The aromatic compounds were obtained from the ZINC database (http://zinc.docking.org/substances/home/) [40] and used for the molecular docking studies in Chimera (version 1.14) by modifying the SDF extension to mol2 in each file. Also, SMILES codes were obtained from the Pubchem database for drawing the chemical structures in Mcule software version 2022. Furthermore, all molecules were prepared on Chimera (Autodock Vina tool) and Mcule softwares (1 click-docking) based on the molecular docking protocol [24,25]. SMILES codes of the ten aromatic compounds obtained from the PubChem database are summarized below: ferulic acid (COc1cc(/C=C/C(=O)O)ccc1O), vanillic acid (COc1cc(C(=O)O)ccc1O), vanillic alcohol (COc1cc(CO)ccc1O), 4-hydroxybenzoic acid (O=C(O)c1ccc(O)cc1), 4-hydroxy cinnamic acid (C1=CC(=CC=C1C=CC(=O)O)O), catechol (C1=CC=C(C(=C1)O)O), eugenol (C=CCc1ccc(O)c(OC)c1), isoeugenol (C/C=C\c1ccc(O)c(OC)c1), 4-Hydroxybenzaldehyde (O=Cc1ccc(O)cc1), protocatechuic acid methyl ester (COC(=O)C1=CC(=C(C=C1)O)O). While the molecules C_4-AHL (CCCC(=O)NC1CCOC1=O), C_{10}-AHL; (CCCCCCCCCC(=O)NC1CCOC1=O), C_{12}-AHL (CCCCCCCCCC(=O)CC(=O)N[C@H]1CCOC1=O), furanone C30 (C1=C(/C(=C/Br)/OC1=O)Br) and vanillin (COc1cc(C=O)ccc1O) were taken as the controls of the molecular dockings. Finally, the results of the molecular dockings were obtained using Chimera (version 14.1) and Discovery Studio (version 2020) softwares [24,32].

Pharmacokinetic and physicochemical characteristics of ligands

The best inhibitors were chosen based on the ΔG values obtained from the molecular docking test. Subsequently, the pharmacokinetic and physicochemical characteristics predictions were made considering the toxicity parameters of each compound by a parameter known as ADME (Absorption, Distribution, Metabolism, and Excretion), which was obtained from the SwissADME online database (http://www.swissadme.ch/) [26]. The protocol used in this study included the use of SMILES codes for each molecule to obtain different pharmacokinetics and toxicity parameters, such as gastrointestinal absorption (GI absorption), blood-brain barrier permeability (BBB permeability), inhibition value for glycoprotein-P 1 (P-gp), as well as inhibitory activity values of the enzyme cytochrome oxidase (CYP) and its variants CYP1A2, CYP2C19, CYP2C9, CYP2D6, and CYP3A4. Additionally, the PubChem database was used for collecting specific physicochemical parameters of each of the selected aromatic compounds [27,41,42]. Finally, the toxicity of each molecule was determined using the database for chemical toxicity prediction (ProTox-II) https://tox-new.charite.de/protox_II/index.php?site=compound_input) [43].

The lethal dose in mice (LD_{50})

The toxicity of aromatic compounds in the mice model was predicted using the toxicity estimation program or T.E.S.T version 4.2.1 (Toxicity Estimation Program Tool). The methodology was based on toxicity estimates from several Quantitative Structure-Activity Relationship (Q.S.A. R) methodologies, such as (a) the hierarchical method, where the toxicity estimate for a drug was obtained using an average value of predictions from various mathematical models. Subsequently, an algorithm-based technique was used to generate models for each aromatic compound to bring the toxicity value. (b) The FDA method predicts a model that looks for chemicals like the test compound. (c) The Nearest Neighbor method uses the expected toxicity of known chemical compound toxicity is estimated by calculating the mean of three substances that are similar to the test substance. All necessary molecular descriptors were calculated within the T.E.S.T. version 4.2.1 tool (https://www.epa.gov/chemicalresearch/toxicity-estimation-programa-tooltest) [44]. Finally, the average LD_{50} value in mice was reported in mg/kg with an acceptable determination coefficient (R^2), utilizing the linear regression from the mathematical models created for each of the analyzed molecules [27,44].

Data analysis

The BGE and LD_{50} in mice were considered variation resources. The results were analyzed using a model equivalent to the completely randomized balanced analysis. The comparison of means among treatments was carried out by using the Tukey test ($p \leq 0.05$). Statistical analysis was performed with the Minitab 2020 program [45]. All results are presented in the means of the replicates obtained by Mcule, Chimera, T.E.S.T. 4.2.1, and NAMD softwares.

Method validation

As the three-dimensional structure model of the QS transcriptional regulator of *P. aeruginosa* (RhlR) is not registered in the PDB database, the three-dimensional structure model was constructed based on a homology model using the SWISS-MODEL server and was obtained ten three-dimensional structure models for the transcriptional regulator. The best model was selected using the three-dimensional structure model of the SdiA transcriptional regulator (PDB: 4y15.2.A) as a template, with a 40.5% identity and a coverage of 0.96 (Fig. 1A), and QMEAN values of Z= -2.09. This three-dimensional structure model was considered suitable because a "QMEAN" Z-score value below -4.0 indicates low quality [23,46]. On the other hand, the values obtained from GMQE (0.75±0.05) and global QMEANDisCo (0.78±0.05) were considered good quality values for the RhlR three-dimensional structure model because both values describe the quality of the model, considering between 0 and 1 score values, where the highest values indicate the best quality [47].

Additionally, the three-dimensional structure model of the transcriptional regulators SdiA and RhlR were analyzed in the ProSA server; the Z-score value for the template SdiA (PDB: AY15) was -7.75, while for the RhlR model was -7.82. Then the RhlR three-dimensional structure model generated by SWISS-MODEL shows a similar value to the three-dimensional structure model of SdiA, validating the quality of the three-dimensional structure models (Fig. 1B and D) [48]. Finally, the Ramachandran plot was obtained for each protein (Fig.1C and E).

Molecular docking for the QS transcriptional regulators

The BGE values for each LasR interaction were observed as competitive inhibition when comparing the BGE values between the natural ligand (C_{12}-AHL) and the inhibitor furanone C30. The BGE values for LasR and its natural ligand C_{12}-AHL were -8.02±0.49 and -7.73±0.152 kcal/mol as obtained by Mcule and Chimera software, respectively. BGE value of LasR was close to the results obtained by several authors [49,50]. The molecular docking values were more significant than those obtained for the vanillin (-4.02±0.05 kcal/mol) and furanone C30 (-4.03±0.1 kcal/mol). These molecules were considered for comparison with other aromatic compounds' interactions because both have been experimentally shown to be inhibitors of QS in the genus *Pseudomonas* [14,51].

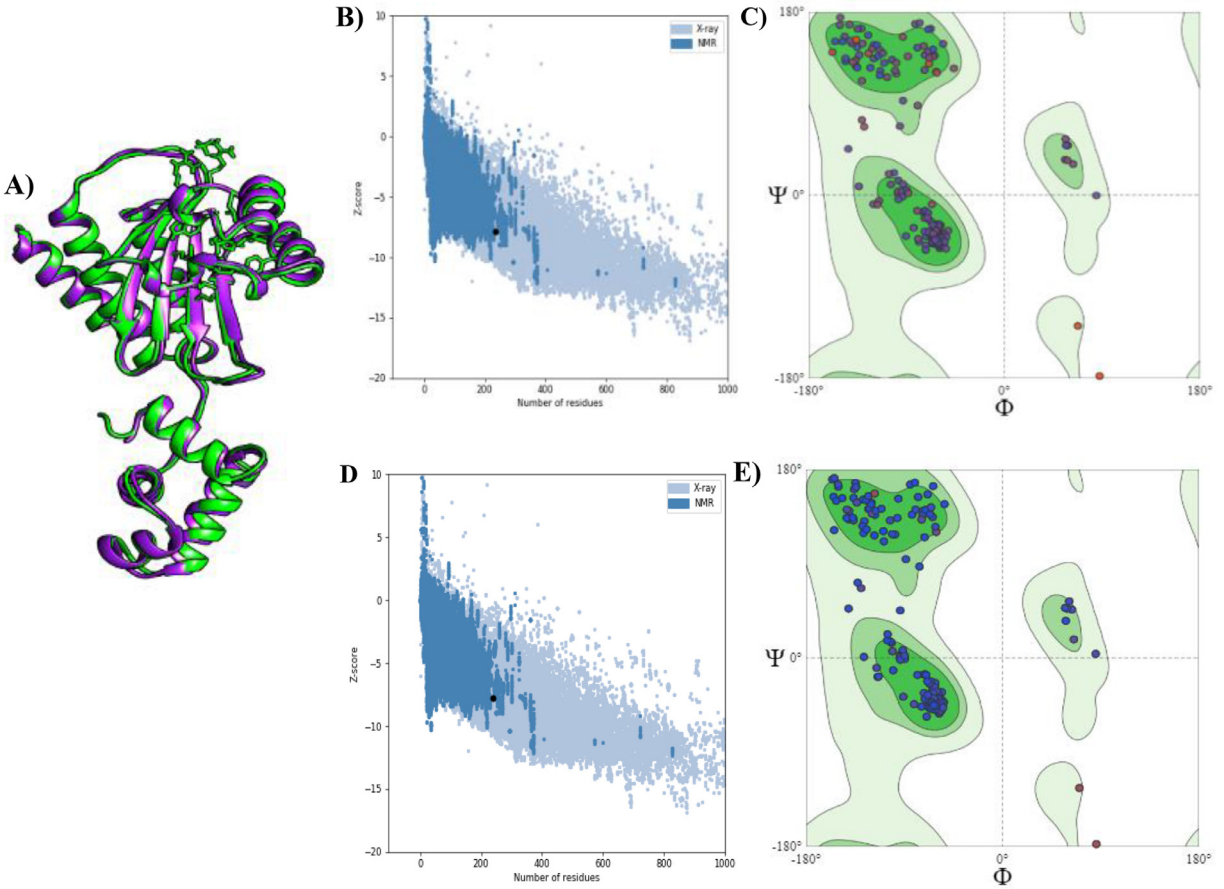

Fig. 1. A) Three-dimensional structure model of transcriptional regulator RhlR matched with SdiA, B) ProSA Z-score of three-dimensional structure model of transcriptional regulator RhlR, C) Ramachandran plot of three-dimensional structure model of transcriptional regulator RhlR, D) ProSA Z-score of three-dimensional structure model transcriptional regulator SdiA, and E) Ramachandran plot of three-dimensional structure model of transcriptional regulator SdiA.

Table 1
The BGE values obtained by molecular docking analysis of aromatic compounds with the autoinducer-1 binding domain of the RhlR transcriptional regulator of *P. aeruginosa*.

Molecule	Mcule (ΔG in -kcal/mol)	Chimera (ΔG in -kcal/mol)
C_4-AHL	-6.53±0.1 ^{BC}	-6.50±0.80 ^{CD}
Furanone C30	-4.30±0.05 ^{A}	-4.50±0.20 ^{A}
Vanillin	-6.20±0.17 ^{B}	-5.87±0.21 ^{BCD}
Catechol	-5.97±0.15 ^{B}	-5.63±0.38 ^{ABC}
Eugenol	**-6.70±0.21** ^{BC}	**-6.87±0.46** ^{CD}
Ferulic acid	**-7.43±0.35** ^{C}	**-7.23±0.15** ^{D}
Hydroxycinnamic acid	**-7.30±0.5** ^{C}	**-7.13±0.51** ^{D}
Hydroxybenzaldehyde	-6.20±0.26 ^{B}	-5.00±0.10 ^{AB}
Isoeugenol	-6.80±0.55 ^{BC}	-5.03±0.38 ^{AB}
Hydroxybenzaldehyde acid	-6.27±0.46 ^{B}	-6.60±0.75 ^{CD}
Protocatechuate	-6.80±0.12 ^{BC}	-6.07±0.45 ^{BCD}
Vanillic acid	-6.67±0.12 ^{BC}	-6.70±0.75 ^{CD}
Vanillic alcohol	-6.13±0.12 ^{B}	-6.87±0.23 ^{CD}

The values are the average standard deviations (n = 3). The bold letters indicate the best results and the different capital letters indicate significant differences in BGE of the methods and microorganisms ($P \leq 0.05$).

Molecular docking analysis of each aromatic compound tested with the LasR regulator from *P. aeruginosa* showed that BGE values ranged from ΔG= -6±0.17 to -7.13±0.21 kcal/mol. Of the ten aromatic compounds analyzed, the highest ΔG values were ferulic acid (-7.13±0.21 kcal/mol), hydroxycinnamic acid (-6.9±0.35 kcal/mol), and protocatechuate (-6.8±0.46 kcal/mol), as calculated using the Mcule software. When the AutoDock Vina method was used with the Chimera software, higher values of ΔG were obtained for the case of ferulic acid (-7.27±0.21 kcal/mol) and hydroxycinnamic acid (-7.03±0.25 kcal/mol). Thus, our results suggest that ferulic acid and hydroxycinnamic acid are the best inhibitors of QS from *P. aeruginosa* (Supplementary Table 1).

Based on the highest average BGE values obtained from both software, the best results for the QscR regulator were ferulic acid, hydroxycinnamic acid, and isoeugenol. (Supplementary Table 2). Finally, the best results obtained for the transcriptional regulator RhlR were ferulic acid, hydroxycinnamic acid, and eugenol were the best inhibitors of the transcriptional regulator RhlR in *P. aeruginosa* (Table 1 displays the most interesting results presented in this section).

The BGE values characterize the interaction of RhlR with its natural ligand (C_4-AHL) with BGE values from aromatic compounds. This showed that the three inhibitors that join more strongly to the autoinducer-1 binding domain are in the transcriptional regulator RhlR, just like the natural ligand, suggesting a competitive inhibition mechanism for the autoinducer-1 binding domain from the transcriptional regulator RhlR.

Fig. 2 shows the best molecular docking results from the interactions for the functional groups of the aromatic compounds with the amino acids located in the autoinducer-1 domain binging of the RhlR transcriptional regulator. These results were compared with the autoinducer-1 binding domain of transcriptional regulator RhlR and the natural ligand (C_4-AHL) (Fig. 2A). This work elucidated the interactions among functional groups of the aromatic compounds with amino acid residues from the autoinducer-1 binding domain of RhlR of *P. aeruginosa* (Fig. 2B). Also, the best aromatic compound interactions with RhlR are ferulic acid, hydroxycinnamic acid, and eugenol (Fig. 2C, E, and G). In addition, Fig. 2D, F, and H display the main interactions of the functional groups (aromatic ring, R-CO, RC-OH, RC=CH_2, R-CH_3, and R-COOH) from ferulic acid, hydroxycinnamic acid, and eugenol with the amino acids of the autoinducer-1 binding domain of RhlR. The interactions between functional groups and amino acid residues differed in each case, mainly consisting of Van der Waals interactions, conventional hydrogen bond, pi-sigma, pi-pi, and pi-alkyl.

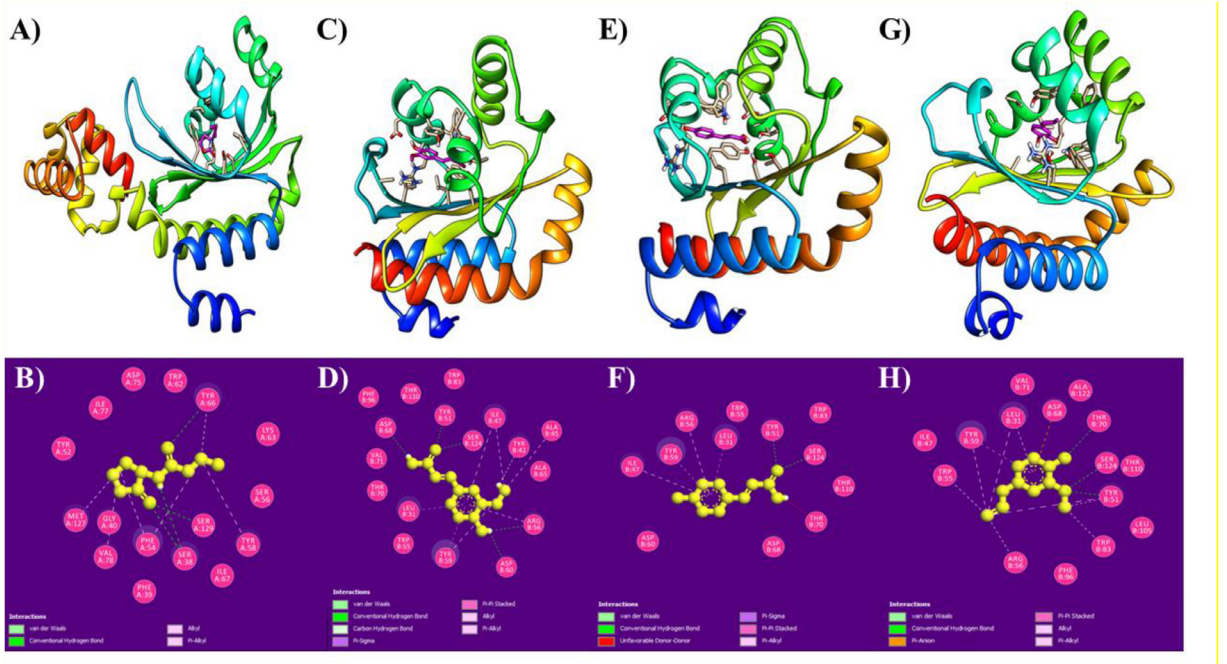

Fig. 2. The best results of molecular docking in RhlR transcriptional regulator of QS of *P. aeruginosa*. A) Molecular docking of C_4-AHL and RhlR, B) C_4-AHL and RhlR interactions, C) molecular docking of ferulic acid and RhlR, D) ferulic acid and RhlR interaction, E) molecular docking of hydroxycinnamic acid and RhlR, F) hydroxycinnamic acid and RhlR interactions, G) molecular docking of eugenol and RhlR and H) eugenol and RhlR interactions. The results were visualized in the Pymol and Discovery studio 2020 software.

Pharmacokinetic studies

The analysis of the best ligands resulting from the molecular docking test showed that the three aromatic compounds matched Lipinski's Rule of Five. Moreover, physicochemical characteristics were similar to the aromatic compounds because they are unsaturated and lipolytic molecules, according to the radar diagrams found in the SwissADME database. Finally, the skin permeation or log Kp varied from -5.69 to -6.41 cm/s in the three aromatic compounds (ferulic acid, hydroxycinnamic acid, and eugenol) obtained from the molecular docking test.

On the other hand, characterization of the inhibitory compounds was essential to know if the aromatic compounds are substrates of the permeability glycoprotein (P-gp) because the crucial role of P-gp is to protect the central nervous system (CNS) from xenobiotics [26,27]. According to the predictive analysis of the human intestinal absorption (HIA) and blood-brain barrier (BBB) permeation, both consisting in the readout of the BOILED-Egg model, all the tested compounds from this study were highly absorbed by the intestine and were skin permeable (Supplementary Table 3).

In addition, the interaction of aromatic compounds with cytochrome oxidase P450 (CYP) was evaluated because it has considered a key player in drug elimination through metabolic biotransformation. In the present study, it was observed that all the values for CYP were the same, showing no inhibition, except for eugenol, which inhibited cytochrome oxidases CYP1A2 and CYP2C. The inhibition of these isoenzymes is undoubtedly one major cause of drug-drug interactions that leads to toxic or other unwanted adverse effects due to the lesser clearance and accumulation of the drug or its metabolites. Numerous inhibitors of the CYP isoforms have been identified, some affecting different CYP isoforms, while others show selectivity for specific isoenzymes. Therefore, it is of great importance for drug discovery to predict the propensity that molecules possess to cause significant drug interactions through inhibition of CYPs and to determine which isoforms are affected [26,27].

LD_{50} studies on mice

Pre-clinical studies in mice are essential to know the effect of a drug in an animal model. On many occasions, the software is helpful to know the doses at which certain substances may be harmful before transferring the experiments from *in vitro* to *in vivo* studies [51]. In the present study, a prediction was made by QSAR methods using mice to obtain LD_{50} values (mg/kg) of aromatic compounds administered orally. The best results were for ferulic acid, hydroxycinnamic acid, and eugenol compared with the inhibitors of QS (vanillin and furanone C30), and the LD_{50} values were close to those experimentally obtained for each compound [52–56]. Finally, regarding the toxicity analysis, all the compounds were non-toxic, except for ferulic acid, which presented high immunotoxicity (Supplementary Table 3).

Molecular dynamics

The results of the root mean square deviation (RMSD) were obtained while simulating the three interactions of aromatic compounds and RhlR. The stability of the interactions of ferulic acid and RhlR were obtained at 5 ns with a mean of 2.27447±0.256 Å. At the same time, the interaction of hydroxycinnamic acid and RhlR was stable at 10 ns with a mean of 2.293±0.2 Å. Finally, the eugenol and RhlR were stable at 7.5 ns with a mean of 2.370±0.25 Å (Fig. 3A, B, and C). In addition, when analyzing the results of RMSF distance values, observing similarity in the high distance peaks in certain amino acids during the interaction protein-ligand. The ferulic acid showed seven peaks of the entire length of the RhlR protein (1, 37-41, and 43) (Supplementary Fig. 1A). In comparison, the interaction with hydroxycinnamic acid showed eleven peaks of the entire length of the RhlR protein (1, 37-44, 116, and 162) (Supplementary Fig. 1B). Finally, when the eugenol interaction was analyzed, nine peaks of the entire length of the RhlR protein (1, 9, 40-44, 86, and 162) (Supplementary Fig. 1C).

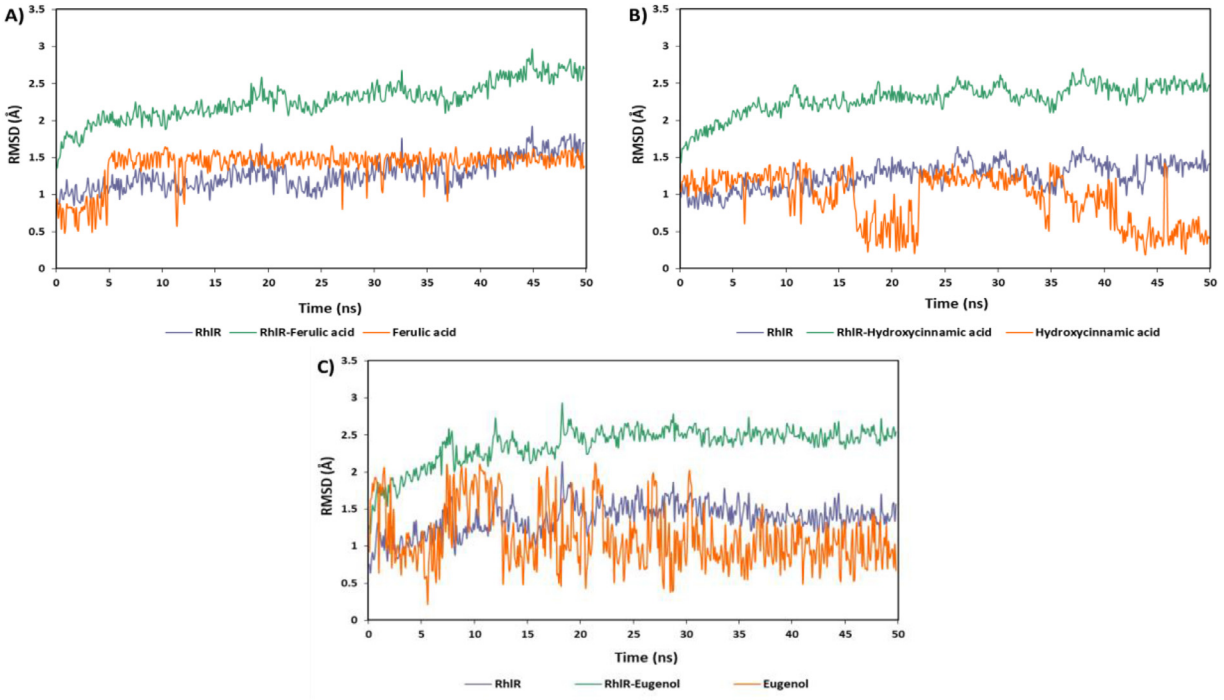

Fig. 3. The RMSD values of the best interactions of inhibitors of the transcriptional regulator RhlR. A) RMSD values for RhlR and ferulic acid complex, B) RMSD values for RhlR and hydroxycinnamic acid complex, and C) RMSD values for RhlR and eugenol complex.

Table 2
The stability binding free energy by molecular mechanics/generalized Born surface area (MM/GBSA).

Complex protein-ligand	Dynamic molecular software/force field	Simulation box dimensions (x, y, and z)	Number of neutralizing ions	Stability	ΔGbind[a] (kJ/mol)	ΔGvdW[a] (kJ/mol)	References
RhlR and natural ligand C_4-AHL	Gromacs 5.0/CHARMM27	No data	No data	Stable	-31.078±2.794 to -44.52 (no statistical difference reported)	-115.34 (no statistical difference reported) to -138.64 ±0.857	[57,58]
RhlR and ferulic acid	NAMD 2.13/CHARMM27	99.11, 95.18 and 114.83	6 Na^+	Stable	**-75.07±0.892**	-97.34± 0.32	This work
RhlR and eugenol	NAMD 2.13/CHARMM27	99.11, 95.18 and 114.83	6 Na^+	Stable	**-70.36± 1.022**	-110.45± 0.52	This work
RhlR and hydroxycinnamic acid	NAMD 2.13/CHARMM27	99.11, 95.18 and 114.83	6 Na^+	Stable	-58.86± 0.90	-87.77± 0.42	This work

[a] The BGE (ΔGbind) and [a] Van der Waals energy (ΔGvdW). The bold letters indicate the best results.

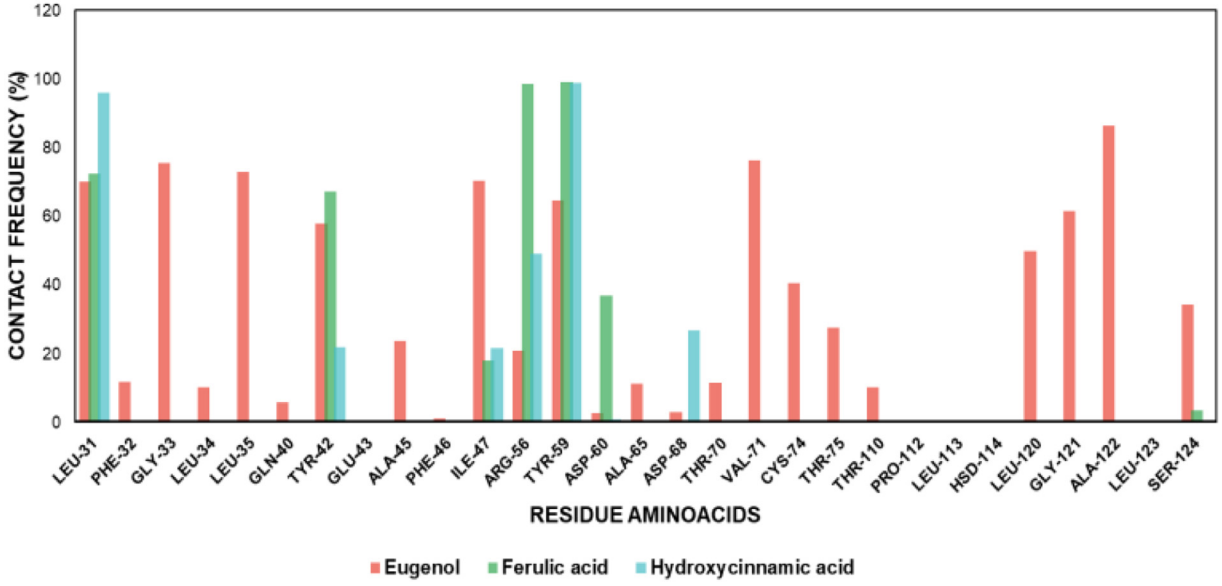

Fig. 4. Contact frequency of amino acids located in the autoinducer-1 binding domain of RhlR in the protein-ligand interactions (RhlR and eugenol, RhlR and ferulic acid, and RhlR and hydroxycinnamic acid).

Frequency of use of amino acids

Some amino acids were frequently found in each interaction, as shown in Fig. 4. In addition, it was observed that amino acids, such as Leu31, Tyr42, Lle47, Arg56, and Tyr59, were commonly used by all three ligands when interacting with the autoinducer-1 binding domain of RhlR (Fig. 4). These results contrasted with molecular docking results (Fig. 2D, F, and H). These amino acids were also found during the interaction of ligand natural C_4-AHL with the autoinducer-1 binding domain of RhlR, which suggests a similar binding mechanism of aromatic compounds and C_4-AHL with the transcriptional regulator of QS in *P. aeruginosa*.

On the other hand, the solvent-accessible surface area (SASA) values of amino acid residues involved in the binding to the autoinducer-1 binding domain in the transcriptional regulator RhlR showed similarly mean SASA values: RhlR and eugenol (9488.923±182.914 Å2), RhlR and ferulic acid (9681.240±177.17 Å2) and RhlR and hydroxycinnamic acid (9505.872±179.12 Å2). Observe an increase in amino acid flexibility in the autoinducer binding domain with ferulic acid compared with hydroxycinnamic acid and eugenol (Supplementary Fig. 2A, 2B, and 2C).

On the other side, the solvent-accessible surface area (SASA) values of amino acid residues involved in the binding to the autoinducer-1 binding domain in the transcriptional regulator RhlR showed similarly average SASA values; RhlR and eugenol (9488.923±182.914 $Å^2$), RhlR and ferulic acid (9681.240±177.17 $Å^2$) and RhlR and hydroxycinnamic acid (9505.872±179.12 $Å^2$). An increase in the flexibility of amino acids in the autoinducer binding domain with ferulic acid compared with hydroxycinnamic acid and eugenol was observed (Supplementary Fig. 2A, 2B, and 2C).

MM/GBSA test

Finally, the total BGE by molecular mechanics/generalized Born surface area (MM/GBSA) was analyzed, and the results for each compound were observed in Table 2. Demonstrated that three inhibitors are stable with their neutralized ions and found that the inhibitors as the ferulic acid and eugenol produced the highest total binding energy (ΔG bind= -75.07±0.892 and -70.36±1.022 kJ/mol, respectively) from three compounds tested. The compounds bound most strongly and significantly to the autoinducer-1 binding domain in RhlR compared with the natural ligand C_4-AHL (ΔGbind= -31.078±2.794 kJ/mol), showing that both molecules exhibit a high potential to bind to QS transcriptional regulator RhlR in *P. aeruginosa*.

Conclusion

Of the ten aromatic compounds tested in the present study by molecular docking, ferulic acid and eugenol showed the best binding BGE values. Also, the *in silico* studies validated the molecular docking using the molecular dynamics test using a reproducible and valuable protocol with different software such as Mcule, Chimera, and NAMD. With the use of defined putative QS inhibitors of RhlR, the transcriptional regulator of QS, proposing the combining ferulic acid and eugenol as a new therapy against virulent *P. aeruginosa* for derived further research from the present study.

Declaration of Competing Interest

The author declares that they have no known competing financial interests or personal relationships that could have appeared to influence the work reported in this paper.

Data availability

No data was used for the research described in the article.

Supplementary materials

Supplementary material associated with this article can be found, in the online version, at doi:10.1016/j.mex.2022.101771.

References

[1] G. Bodelón, V. Montes-García, V. López-Puente, E.H Hill, C. Hamon, M.N Sanz-Ortiz, L.M Liz-Marzán, Detection and imaging of quorum sensing in *Pseudomonas aeruginosa* biofilm communities by surface-enhanced resonance Raman scattering, Nat. Mater. 15 (11) (2016) 1203-1211, doi:10.1038/nmat4720.

[2] Y.C. Liu, K.G. Chan, C.Y. Chang, Modulation of host biology by *Pseudomonas aeruginosa* quorum sensing signal molecules: messengers or traitors, Front. Microbiol. 9 (6) (2015) 1–9 0.3389/fmicb.2015.01226.

[3] A. Rajput, K.M. Kaur, Kumar. SigMol: repertoire of quorum sensing signaling molecules in prokaryotes, Nucleic Acids Res 44 (1) (2016) 634–639, doi:10.1093/nar/gkv1076.

[4] H. Chen, A. Li, C. Cui, F. Ma, D. Cui, H. Zhao, J. Yang, AHL-mediated quorum sensing regulates the variations of microbial community and sludge properties of aerobic granular sludge under low organic loading, Environ. Int. 130 (2019) 1–13, doi:10.1016/j.envint.2019.104946.

[5] R.L Cruz, k.L. Asfahl, S. Van den Bossche, T. Coenye, A. Crabbé, A.A. Dandekar, RhlR-regulated acyl-homoserine lactone quorum sensing in a cystic fibrosis isolate of *Pseudomonas aeruginosa*, MBio 11 (2) (2020) 1–14, doi:10.1128/mBio.00532-20.

[6] S. Yan, G. Wu, Can biofilm be reversed through quorum sensing in *Pseudomonas aeruginosa*? Front. Microbiol. 10 (1582) (2019) 1–9, doi:10.3389/fmicb.2019.01582.

[7] S. Mathew, T.E. Abraham, Bioconversions of ferulic acid, an hydroxycinnamic acid, Crit. Rev. Microbiol. 32 (2006) 115–125, doi:10.1080/10408410600709628.

[8] N. Ito, M. Itakura, S. Eda, K. Saeki, H. Oomori, T. Yokoyama, K. Minamisawa, Global gene expression in *Bradyrhizobium japonicum* cultured with vanillin, vanillate, 4-hydroxybenzoate and protocatechuate, Microbes Environ 21 (2006) 240–250, doi:10.1264/jsme2.21.240.

[9] N.A. Zamzuri, S. Abd-Aziz, R.A. Rahim, L.Y. Phang, N.B. Alitheen, T. Maeda, A rapid colorimetric screening method for vanillic acid and vanillin-producing bacterial strains, J. Appl. Microbiol. 116 (4) (2014) 116 903–10, doi:10.1111/jam.12410.

[10] V. Paul, D.C. Rai, R.L. TS, S.K. Srivastava, A.D. Tripathi, A comprehensive review on vanillin: its microbial synthesis, isolation and recovery, Food Biotechnol 35 (1) (2021) 22–49, doi:10.1080/08905436.2020.1869039.

[11] FDA page. Available in: https://www.accessdata.fda.gov/scripts/cdrh/cf docs/cfcfr/CFRSearch.cf. Revisada en 5 de febrero del 2021.

[12] J.H. Choo, Y. Rukayadi, J.K. Hwang, Inhibition of bacterial quorum sensing by vanilla extract, Lett. Appl. Microbiol. 42 (2006) 637–641 0.1111/j.1472-765X.2006.01928.x.

[13] M. Lemos, A. Borges, J. Teodósio, P. Araújo, F. Mergulhão, L. Melo, M. Simões, The effects of ferulic and salicylic acids on *Bacillus cereus* and *Pseudomonas fluorescens* single-and dual-species biofilms, Int. Biodeterior. Biodegrad. 86 (2014) 42–51, doi:10.1016/j.ibiod.2013.06.011.

[14] A. Ugurlu, A.K. Yagci, S. Ulusoy, B. Aksu, G. Bosgelmez-Tinaz, Phenolic compounds affect production of pyocyanin, swarming motility and biofilm formation of *Pseudomonas aeruginosa*. Asian Pac, J. Trop. Biomed. 6 (2016) 698–701, doi:10.1016/j.apjtb.2016.06.008.

[15] G.R. Gandhi, A.B.S. Vasconcelos, G.H. Haran, D.A. Silva, V.K. Calisto, G. Jothi, J.D.S.S. Quintans, R.Q. Gurgel, Essential oils and its bioactive compounds modulating cytokines: A systematic review on anti-asthmatic and immunomodulatory properties, Phytomedicine 73 (2019) 1–37, doi:10.1016/j.phymed.2019.152854.

[16] D.P. Ramadoss, N. Sivalingam, Vanillin extracted from *Proso* and *Barnyard millets* induce apoptotic cell death in HT-29 human colon cancer cell line, Nutr. Cancer. 72 (2020) 1422–1437, doi:10.1080/01635581.2019.1672763.

[17] A. Chang, S. Sun, L. Li, X. Dai, H. Li, Q. He, H. Zhu, Tyrosol from marine Fungi, a novel Quorum sensing inhibitor against *Chromobacterium violaceum* and *Pseudomonas aeruginosa*, Bioorg. Chem. 91 (2019) 1–28, doi:10.1016/j.bioorg.2019.103140.

[18] Y. Chang, P.C. Wang, H.M. Ma, S.Y. Chen, Y.H. Fu, Y.Y. Liu, P.H. Sun, Design, synthesis and evaluation of halogenated furanone derivatives as quorum sensing inhibitors in *Pseudomonas aeruginosa*, Eur J Pharm Sci 140 (2019) 1–44, doi:10.1016/j.ejps.2019.105058.

[19] D. Deryabin, K. Inchagova, E. Rusakova, G. Duskaev, Coumarin's anti-quorum sensing activity can be enhanced when combined with other plant-derived small molecules, Molecules 26 (2021) 1–10, doi:10.3390/molecules26010208.

[20] S. Manner, A. Fallarero, Screening of natural product derivatives identifies two structurally related flavonoids as potent quorum sensing inhibitors against gram-negative bacteria, Int. J. Mol. Sci. 19 (2018) 1–18 0.3390/ijms19051346.

[21] F.G. Martins, A. Melo, S.F. Sousa, Identification of new potential inhibitors of quorum sensing through a specialized multi-level computational approach, Molecules 26 (9) (2021) 1–21, doi:10.3390/molecules26092600.

[22] J.E. Paczkowski, A.R. McCready, J.P. Cong, Z. Li, P.D. Jeffrey, C.D. Smith, B.L. Bassler, An autoinducer analogue reveals an alternative mode of ligand binding for the LasR quorum-sensing receptor, ACS Chem. Biol. 14 (3) (2019) 378–389, doi:10.1021/acschembio.8b00971.

[23] A. Waterhouse, M. Bertoni, S. Bienert, G. Studer, G. Tauriello, R. Gumienny, T. Schwede, SWISS-MODEL: homology modelling of protein structures and complexes, Nucleic Acids Res 46 (1) (2018) 296–303, doi:10.1093/nar/gky427.

[24] S.S. Butt, Y. Badshah, M. Shabbir, M. Rafiq, Molecular docking using chimera and autodock vina software for nonbioinformaticians, JBB 1 (1) (2020) 1–25, doi:10.2196/14232.

[25] H.A. Odhar, A.M. Rayshan, S.W. Ahjel, A.A. Hashim, A.A.M.A. Albeer, Molecular docking enabled updated screening of the matrix protein VP40 from Ebola virus with millions of compounds in the MCULE database for potential inhibitors, Bioinformation 15 (2019) 1–6, doi:10.6026/97320630015627.

[26] A. Daina, O. Michielin, V. Zoete, SwissADME: a free web tool to evaluate pharmacokinetics, drug-likeness and medicinal chemistry friendliness of small molecules, Sci. rep. 7 (1) (2017) 1–13, doi:10.1038/srep42717.

[27] A. Talevi, *in silico* ADME: Rule-Based Systems, in: The ADME Encyclopedia: A Comprehensive Guide on Biopharmacy and Pharmacokinetics, Springer International Publishing, 2021, pp. 1–7. 10.1007/978-3-030-51519-5_148-1.

[28] A. Panwar, A. Kumar, *In-silico* analysis and molecular dynamics simulations of lysozyme by GROMACS 2020.2, Ann. Rom. Soc. Cell Biol. 25 (6) (2021) 9679–9685.

[29] J.C. Phillips, D.J. Hardy, J.D. Maia, J.E. Stone, J.V. Ribeiro, R.C. Bernardi, E. Tajkhorshid, Scalable molecular dynamics on CPU and GPU architectures with NAMD, J. Chem. Phys. 153 (4) (2020) 1–34, doi:10.1063/5.0014475.

[30] T. Hou, J. Wang, Y. Li, W. Wang, Assessing the performance of the MM/PBSA and MM/GBSA methods. 1. The accuracy of binding free energy calculations based on molecular dynamics simulations, J. Chem. Inf. Model. 51 (2011) 69–82, doi:10.1021/ci100275a.
[31] S. Yuan, H.S Chan, Z. Hu, Using PyMOL as a platform for computational drug design, Wiley Interdisciplinary Reviews: Computational Molecular Science 7 (2) (2017) 1–10, doi:10.1002/wcms.1298.
[32] B.L. Jejurikar, S.H Rohane, Drug designing in discovery studio, Asian J. Res. Chem. 14 (2) (2021) 135–138, doi:10.5958/0974-4150.2021.00025.0.
[33] W. Wang, M. Xia, J. Chen, F. Deng, R. Yuan, X. Zhang, F. Shen. Data set for phylogenetic tree and RAMPAGE Ramachandran plot analysis of SODs in *Gossypium raimondii* and *G. arboreum*. Data Brief. 9 (2016) 345-348. 10.1016/j.dib.2016.05.025.
[34] M. Wiederstein, M.J. Sippl, ProSA-web: interactive web service for the recognition of errors in three-dimensional structures of proteins, Nucleic Acids Res 35 (2) (2007) 407–410, doi:10.1093/nar/gkm290.
[35] B. Webb, A. Sali, Protein structure modeling with MODELLER, in: Structural Genomics, Humana, New York, NY, 2021, pp. 239–255, doi:10.1007/978-1-4939-0366-5_1.
[36] R.A. Laskowski, J.M.Thornton M.W.MacArthur, PROCHECK: validation of protein-structure coordinates, Internat. Tables Crystallogr. 21 (2006) 684–687, doi:10.1107/97809553602060000882.
[37] A. Vetrivel, S. Natchimuthu, V. Subramanian, R. Murugesan, High-throughput virtual screening for a new class of antagonist targeting LasR of *Pseudomonas aeruginosa*, ACS omega 6 (28) (2021) 18314–18324, doi:10.1021/acsomega.1c02191.
[38] K. Ponnusamy, S. Kappachery, M. Thekeettle, J.H Song, J.H Kweon, Anti-biofouling property of vanillin on *Aeromonas hydrophila* initial biofilm on various membrane surfaces, World J. Microbiol. Biotechnol. 29 (9) (2013) 1695–1703, doi:10.1007/s11274-013-1332-2.
[39] V. Markus, K. Golberg, K. Teralı, N. Ozer, E. Kramarsky-Winter, R.S. Marks, A. Kushmaro, Assessing the molecular targets and mode of action of furanone C-30 on *Pseudomonas aeruginosa* quorum sensing, Molecules 26 (6) (2021) 1–14, doi:10.3390/molecules26061620.
[40] J.J. Irwin, B.K. Shoichet, ZINC– a free database of commercially available compounds for virtual screening, J. Chem. Inf. Model. 45 (1) (2005) 177–182, doi:10.1021/ci049714.
[41] H.A. Odhar, S.W. Ahjel, A.A.M. A.Albeer, A.F Hashim, A.M Rayshan, S.S Humadi, Molecular docking and dynamics simulation of FDA approved drugs with the main protease from 2019 novel coronavirus, Bioinformation 16 (3) (2020) 236–244, doi:10.6026/97320630016236.
[42] S. Kim, J. Chen, T. Cheng, A. Gindulyte, J. He, S. He, E.E Bolton, PubChem 2019 update: improved access to chemical data, Nucleic Acids Res 47 (2019) 1102–1109, doi:10.1093/nar/gky1033.
[43] S. Ghosh, P. Tripathi, P. Talukdar, S.N. Talapatra, *In silico* study by using ProTox-II web server for oral acute toxicity, organ toxicity, immunotoxicity, genetic toxicity endpoints, nuclear receptor signalling and stress response pathways of synthetic pyrethroids, WSN (2019) 35–51, doi:10.1093/nar/gky318.
[44] P. Ruiz, G. Begluitti, T. Tincher, J. Wheeler, M. Mumtaz, M. Prediction of acute mammalian toxicity using QSAR methods: a case study of sulfur mustard and its breakdown products, Molecules 17 (8) (2012) 8982–9001, doi:10.3390/molecules17088982.
[45] A. Alin, Minitab, Wiley Interdiscip Rev. Comput. Stat. 2 (6) (2010) 723–727, doi:10.1002/wics.113.
[46] P. Benkert, M. Biasini, T. Schwede, Toward the estimation of the absolute quality of individual protein structure models, Bioinformatics 27 (2011) 343–350, doi:10.1093/bioinformatics/btq662.
[47] G. Studer, C. Rempfer, A.M Waterhouse, R. Gumienny, J. Haas. Schwede, QMEANDisCo-distance constraints applied on model quality estimation, Bioinformatics 36 (2020) 1765–1771, doi:10.1093/bioinformatics/btz828.
[48] N. Chowdhury, A. Bagchi, Identification of ligand binding activity and DNA recognition by RhlR protein from opportunistic pathogen *Pseudomonas aeruginosa* a molecular dynamic simulation approach, J. Mol. Recognit. 31 (12) (2018) 1–7, doi:10.1002/jmr.2738.
[49] A. Annapoorani, V. Umamageswaran, R. Parameswari, S.K Pandian, A.V Ravi, Computational discovery of putative quorum sensing inhibitors against LasR and RhlR receptor proteins of *Pseudomonas aeruginosa*, J. Comput. Aided Mol. Des. 26 (9) (2012) 1067–1077, doi:10.1007/s10822-012-9599-1.
[50] A Corral-Lugo, A. Daddaoua, A. Ortega, M. Espinosa-Urgel, T. Krell, Rosmarinic acid is a homoserine lactone mimic produced by plants that activates a bacterial quorum-sensing regulator, Sci. Signal. 9 (409) (2016) 1–10, doi:10.1126/scisignal.aaa8271.
[51] H. Yu, Y. Liu, F. Yang, Y. Xie, Y. Guo, Y. Cheng, W. Yao, The combination of hexanal and geraniol in sublethal concentrations synergistically inhibits Quorum Sensing of *Pseudomonas fluorescens in vitro* and *in silico* approaches, J. Appl. Microbiol. (2022) 1–15, doi:10.1111/jam.15446.
[52] J.C. Ingvast-Larsson, V.C. Axén, A.K. Kiessling, Effects of isoeugenol on *in vitro* neuromuscular blockade of rat phrenic nerve diaphragm preparations, Am. J. Vet. Res. 64 (6) (2003) 690–693, doi:10.2460/ajvr.2003.64.690.
[53] S. Kegley, E. Konlisk, M. Moses, Marin municipal water district. Herbicide risk assessment. Chapter 6: clove oil (eugenol), Berkeley: pesticide research institute 1 (2010) 1–20.
[54] S.N. Talapatra, A. Sarkar, Acute toxicity prediction of synthetic and natural preservatives in rat by using QSAR modeling software, Int. J. Adv. Res. 3 (7) (2015) 1424–1438.
[55] L. Vijayasteltar, G.G Nair, B. Maliakel, R Kuttan, Safety assessment of a standardized polyphenolic extract of clove buds: subchronic toxicity and mutagenicity studies, Toxicol. Rep. 3 (2016) 439–449, doi:10.1016/j.toxrep.2016.04.001.
[56] V.F. Salau, O.L Erukainure, C.U Ibeji, T.A. Olasehinde, N.A Koorbanally, M.F Islam, Ferulic acid modulates dysfunctional metabolic pathways and purinergic activities, while stalling redox imbalance and cholinergic activities in oxidative brain injury, Neurotox. Res. (2019) 1–12 0.1007/s12640-019-00099-7.
[57] N. Chowdhury, A Bagchi, Identification of ligand binding activity and DNA recognition by RhlR protein from opportunistic pathogen *Pseudomonas aeruginosa* a molecular dynamic simulation approach, J. Mol. Recognit. 31 (12) (2018) 1–7, doi:10.1002/jmr.2738.
[58] N. Chowdhury, A Bagchi, Elucidation of the hetero-dimeric binding activity of LasR and RhlR proteins with the promoter DNA and the role of a specific Phe residue during the biosynthesis of HCN synthase from opportunistic pathogen *Pseudomonas aeruginosa*, J. Mol. Model. 27 (3) (2021) 1–15 0.1007/s00894-021-04701-8.